Effect of Rhenium on the Dislocation Core Structure in Tungsten

Lorenz Romaner,[1,2,*] Claudia Ambrosch-Draxl,[2] and Reinhard Pippan[1]

[1]*Erich Schmid Institute of Materials Science, Austrian Academy of Sciences, Jahnstrasse 12, A-8700 Leoben, Austria*
[2]*Chair of Atomistic Modelling and Design of Materials, University of Leoben, Franz-Josef-Straße 18, A-8700 Leoben, Austria*

(Received 7 June 2009; published 13 May 2010)

Despite exhibiting the highest melting point of all metals, the technological use of tungsten is hampered by its room-temperature brittleness. Alloying with Re significantly ductilizes the material which has been assigned to modified properties of the $1/2\langle 111\rangle$ screw dislocation. Using density functional theory, we show that alloying induces a transition from a symmetric to an asymmetric core and a reduction in Peierls stress. This combination ductilizes the alloy as the number of available slip planes is increased and the critical stress needed to start plastic deformation is lowered.

DOI: 10.1103/PhysRevLett.104.195503 PACS numbers: 61.66.Dk, 31.15.es, 61.72.Lk, 62.20.F−

Tungsten is the metal with the highest melting point and is of prominent importance for technological applications where components are facing high temperatures. A major drawback in this connection is, however, the room-temperature brittleness which imposes severe limits on the formability of this material and its resistance to mechanical load. This problem is common to all the group VIA metals, tungsten, molybdenum, and chromium, and it has been long recognized that it can be decisively reduced by alloying with rhenium [1,2]. Despite the big technological relevance of this ''Re ductilizing effect'' its application is limited by the fact that Re is a very rare metal. Hence, to achieve the same result with alternative elements or methods, a full understanding of this effect is inevitable.

The physical origins behind the Re-induced ductilization have been heavily debated and several possible mechanisms have been discussed [2–5]. Among these, (i) solid solution softening which is supposed to originate from an improved mobility of $1/2\langle 111\rangle$ screw dislocations [3,6,7] and (ii) change in slip plane from {110} to {112} [4,8], play a key role, as the former reduces the critical stress level necessary to start plastic deformation while the latter increases the number of available slip planes from 6 to 12. In this Letter, we show that the two effects can be explained based on changes in the interatomic bonding arising from the filling of the d band. Using functional theory (DFT) calculations we demonstrate that, upon alloying, the $1/2\langle 111\rangle$ dislocation exhibits a transition from a symmetric to an asymmetric core which causes the change in preferred slip plane. Furthermore, we prove the softening of the material by direct calculation of the critical stress which has to be applied to move the dislocation at 0 K (Peierls stress σ_P).

W-Re alloys are modeled in two different ways: in the supercell approach, a certain amount of W atoms is substituted by Re atoms at specific atomic sites. Alternatively, we also employ the virtual crystal approximation (VCA) [9] where W and Re atoms are substituted by one effective type of atom of intermediate nuclear and electronic charge. This approach has already been successfully applied to model crystal stability and vibrations in W-Re alloys [10]. The two methods complement each other as the former provides information for a specific Re distribution while the latter mimics an average over many configurations.

VCA calculations are carried out with the QUANTUM-ESPRESSO package [11] using norm conserving pseudopotentials in the Troullier-Martins scheme. They were constructed for the $5d$, $6s$, and $6p$ channels for effective Re concentrations of $c = 0$, 0.12, 0.25, and 0.50. Supercell calculations are performed with the VASP code [12] using the projector augmented plane waves method. The Perdew-Burke-Ernzerhof exchange-correlation functional was used throughout this work. Above $c = 0.25$, the alloy undergoes a phase transition from bcc to a σ phase. We, nevertheless, consider $c = 0.50$ as the bcc lattice is still dynamically stable [10] and the influence of Re is displayed very clearly.

Re is a direct neighbor of W in the periodic table, and its influences on the elastic properties are well established. From considerations based on filling the d band of the transition metals one expects a decrease in lattice parameter a_0 and an increase in bulk modulus, B and elastic anisotropy, A [13]. The latter is defined as $A = C_{44}/C'$ where $C' = 1/2(C_{11} - C_{12})$ and C_{44} are elastic constants which measure the resistance against different types of shear. In Table I these quantities are given as obtained from VCA and supercell calculations. Besides small deviations between the two approaches, both reproduce the expected trend for a_0, B, and A. Hence, the alloying-induced changes in the elastic properties, which are very important for dislocation calculations, are well captured by the present methodology.

To model the $1/2\langle 111\rangle$ screw dislocations, we employ a periodic quadrupole arrangement which has been proven to reliably describe core structures, energies, and Peierls stresses [14–17]. Two dislocations with antiparallel Burgers vector are inserted into unit cells characterized by the following lattice vectors: $\vec{a}_1 = r u_{[11\bar{2}]}$, $\vec{a}_2 = 1/2(r u_{[11\bar{2}]} + s u_{[\bar{1}10]})$, $\vec{a}_3 = u_{[111]}$, where $u_{[11\bar{2}]}$, $u_{[\bar{1}10]}$,

TABLE I. Lattice parameter a_0 (Å), bulk modulus B, shear moduli C' and C_{44} (all moduli in GPa) and anisotropy A as a function of Re concentration c.

	c	a_0	B	C'	C_{44}	A
Experiment [13]	0.00	3.165	316	165	164	0.99
	0.10		321	156	171	1.13
VCA	0.00	3.187	300	160	149	0.93
	0.12	3.177	308	138	144	1.04
	0.25	3.166	317	124	142	1.14
	0.50	3.147	330	117	164	1.41
Supercell	0.00	3.189	303	159	146	0.92
	0.12	3.180	310	139	141	1.01
	0.50	3.153	329	110	170	1.54

and $u_{[111]}$ are basis vectors connecting two atoms of the bcc lattice along the specified direction. The parameters r and s are varied between $r = 3, 5, 7$ and $s = 5, 9, 11$ to explore size effects. The number of atoms in the unit cell are, hence, 45, 135, and 231. The starting dislocation geometry is set up in the energetic most favorable "easy-core" structure and is calculated on the basis of linear isotropic elasticity according to Ref. [16] to ensure a proper regularization of the conditionally convergent sum of displacements. Stress is applied by straining the unit cell, i.e., by modification of $\vec{a}_2$ to $\vec{a}_2' = \vec{a}_2 + f\vec{a}_3$ [15,17]. With $f = 0.5$ no external strain is applied [14,16,17] while smaller values induce ϵ_{yz} strain and, consequently, σ_{yz} stress which, according to the Peach-Köhler force, drives the dislocation along the $[11\bar{2}]$ direction. Note that, in case of anisotropicity, ϵ_{yz} strain induces not just σ_{yz} stress but also σ_{xy} stress which can exert a force on the edge components of the dislocation [18]. However, $\sigma_{xy}/\sigma_{yz} = 0.06$ for the 25% alloy and, hence, this influence is neglected. For each stress level, the structure is relaxed with the DFT codes until forces are smaller than 0.01 eV/Å. A $2 \times 4 \times 8$, $1 \times 2 \times 8$ and $1 \times 2 \times 8$ k-point grid was used for the unit cells containing, 45, 135, and 231 atoms, respectively, and a first order Methfessel-Paxton broadening scheme with 0.2 eV broadening was employed. The plane wave energy cutoff was 16.4 Rydberg for the VASP calculations and 30 Rydberg for the ESPRESSO calculations.

The core structure of the relaxed dislocation under zero applied stress is represented in Fig. 1(a) for the 135-atom unit cell, where the circles represent W atoms as they appear when looking onto the (111) surface. The dislocation geometry is evidenced by a differential displacement map [19]. The length of the arrows is proportional to the relative shift of two neighboring atoms along the surface normal when inserting the dislocation in the perfect crystal. An arrow connecting two neighboring atoms represents a shift of 1/3 Burgers vector. In agreement with recent bond order potential (BOP) calculations for W [20,21] we obtain a symmetric core for all unit cells, i.e., the dislocation

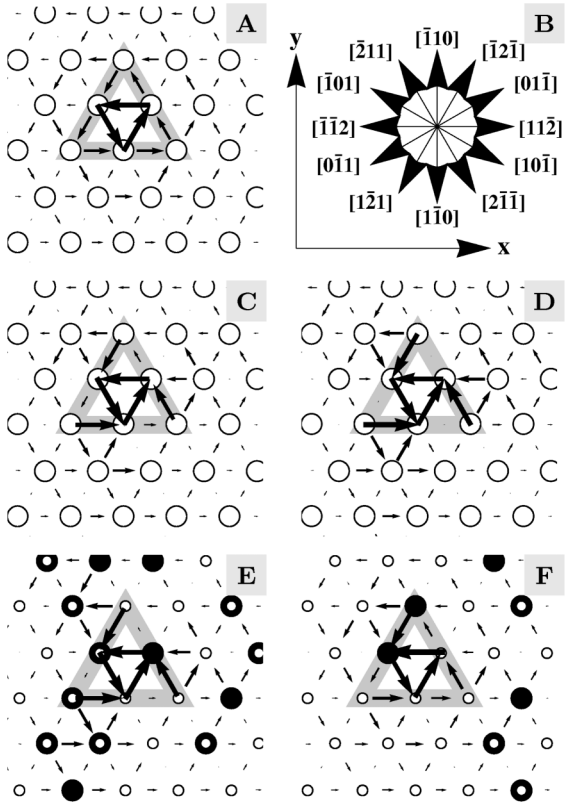

FIG. 1. (a) Illustration of the dislocation structure for $c = 0$. (b) Representation of crystallographic directions. (c) and (d) Dislocation structure for $c = 0.25$ and $c = 0.50$ when using the VCA. (e) and (f) Core structures as obtained from supercell calculations at $c = 0.25$ for different Re distributions (see text). W atoms are illustrated by smaller empty circles while Re atoms are represented by the bigger filled circles.

spreads equally along the six $\langle 112 \rangle$ directions [shown in Fig. 1(b)]. This is most clearly seen by the arrows on the gray triangle being all of equal length.

Alloying with Re leads to changes in interatomic bonding which has decisive consequences for the core structure. As revealed by the VCA calculations at $c = 0.25$ and $c = 0.5$ [Figs. 1(c) and 1(d)] the core displays a pronounced asymmetry in the $\langle 112 \rangle$ directions demonstrating a transition from a symmetric to an asymmetric core structure. The asymmetry is seen to be more pronounced for higher Re content. At $c = 0.12$, an intermediate form of core asymmetry [22] was found as the dislocation is symmetric at zero applied stress but transforms to an asymmetric core when applying stress (smaller than the Peierls stress).

This transition observed with the VCA is confirmed by the supercell calculations. The supercell is built by stacking two 135-atom unit cells (which were used for the VCA calculations) along the [111] direction. Starting from the relaxed structure obtained for $c = 0$, 68 out of the 270 atoms are substituted with Re atoms in random fashion to obtain $c = 0.25$. Then, the geometry is optimized resulting in core structures as illustrated in Figs. 1(e) and 1(f).

Differential displacements are shown for the upper unit cell only as the ones belonging to the lower one are basically identical. The results of two different Re distributions are shown: one, where the core exhibits a higher Re content, and another one where the core is less densely populated by Re. Besides irregularities arising from the random structures, the asymmetric pattern is found in both cores and is more pronounced for the Re-rich core. Hence, whether modeling the alloy in a homogeneous way through the VCA, or when considering specific W-Re configurations by supercell calculations, the transition from a symmetric to an asymmetric core is demonstrated by the present calculations.

Symmetric and asymmetric cores have been discussed extensively in literature [18,19,23,24] and small variations in the description of the interatomic bond can be decisive [25,26]. While empirical potentials predicted an asymmetric core for group VI bcc metals [18,19], BOP [20–22] and DFT calculations [27–29] systematically revealed symmetric core structures. Criteria have been proposed to predict the core structure by means of more basic quantities such as interrow potentials [25] or γ surfaces [18]. The latter is based on the variation in energy when cutting a crystal along the $(\bar{1}10)$ or $(11\bar{2})$ planes and displacing the two parts along the [111] direction. Several works [14,22,24,29] could confirm a criterion which states that the core is asymmetric if $2\gamma(b/6) > \gamma(b/3)$ and symmetric otherwise.

As shown in the Fig. 2(a) the $(\bar{1}10)$ γ surface along the [111] direction as calculated from VCA is reduced for increasing Re concentrations indicative of a pronounced reduction in ideal shear strength. The qualitative shape, however, is remarkably insensitive to c as revealed by Fig. 2(b). Hence, the above mentioned criterion is not satisfied for any concentration up to $c = 0.50$. Analogous observations are made for the $(11\bar{2})$ γ surface (not shown). Thus, the transition observed for the core symmetry is not reflected along the [111] direction of the γ surfaces. However, exploring the full $(\bar{1}10)$ γ surface a clear trend emerges [see Figs. 2(c) and 2(d)]. Close to the minimum (black) the contour plot at $c = 0$ reveals a circular shape while for higher concentrations an elliptical distortion occurs. As has already been pointed out [18] such a feature can be expected to induce a transition from a symmetric to an asymmetric core because of the evolution of strong edge components. Indeed, when performing a structural optimization of the dislocation by fixing the x-y components of the atomic positions, the energetic stabilization in the 135 unit cell gained from the asymmetry at $c = 0.50$ is rather weak, i.e., just 0.02 eV. However, when allowing for edge components, the gain of 0.72 eV is substantial. Hence, we conclude that edge components play a dominant role for the transition from the symmetric to the asymmetric core.

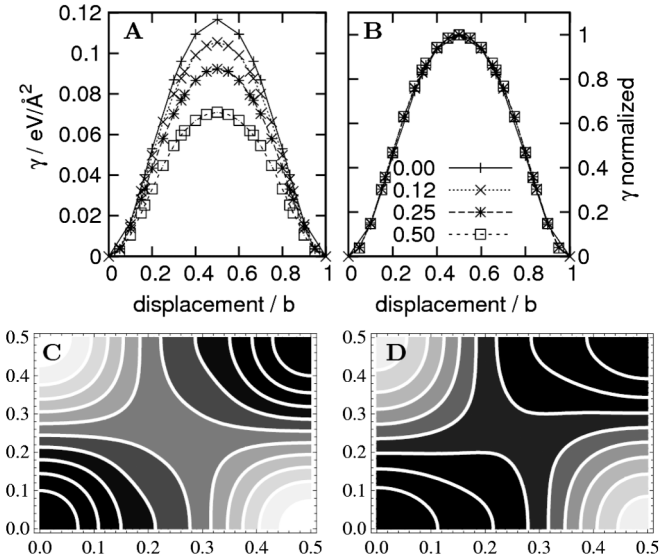

FIG. 2. (a) Illustration of the $(\bar{1}10)$ γ surfaces along the [111] direction for different Re concentrations c. In (b) the curves are normalized. Full $(\bar{1}10)$ γ surfaces at $c = 0$ and $c = 0.5$ are shown in (c) and (d), respectively. The x axis is along the [110] direction while the y axis is along the $[00\bar{1}]$ direction. Contour lines are spaced at 0.022 eV Å^{-2}.

Importantly, this transition has a strong influence on the dislocation slip plane. While symmetric cores move in {110} planes uniformly, asymmetric cores move in these planes in a zigzag manner [23] which changes the overall slip plane to {112}. Indeed, this change in slip plane upon alloying has been observed for all group VI metals [4,8] which is an indirect experimental evidence for this transition and strongly supports our theoretical findings.

Not just the slip plane, but also the Peierls stress σ_P is affected by Re addition. σ_P is calculated as outlined in Refs. [15,17] according to which external stress is applied in discrete steps by straining the unit cell (see above). Small values distort the dislocations reversibly, i.e., when removing the stress the dislocation would return to its original position. When the stress reaches σ_P the dislocation moves irreversibly to a neighboring position. The values obtained for pure W as calculated with VASP are given in Table II together with the error due to discretization $\Delta\sigma_P$. σ_P shows a dependence on unit cell size, comparable to what was found in Ref. [15]. We attribute this dependency to the mutual attraction of the dislocations and

TABLE II. Peierls stress σ_P, error due to discretization $\Delta\sigma_P$ and corrected Peierls stress σ_P^{corr} (all in GPa) for different number of atoms in the unit cell n and Re concentrations c.

n	c	σ_P	$\Delta\sigma_P$	σ_P^{corr}
45	0.00	1.88	0.07	2.85
135	0.00	2.37	0.05	2.75
231	0.00	2.74	0.07	2.88
135	0.00	2.09	0.05	2.49
135	0.12	1.66	0.10	2.09
135	0.25	1.42	0.05	1.84

add this additional contribution σ_s to the externally applied stress. A corrected Peierls stress can, hence, be given as $\sigma_P^{\mathrm{corr}} = \sigma_P + \sigma_s$. We calculate σ_s by differentiating the elastic energy of the periodic dipole structure $E_{\mathrm{el}}(d)$ with respect to the distance d, $\sigma_s = [1/b * \frac{\delta E_{\mathrm{el}}(d)}{\delta d}]_{d=d*}$. The stress is evaluated at the distance where the derivative is assumed to be highest, i.e., $d* = a_0/24^{1/2}$ and $E_{\mathrm{el}}(d)$ is calculated on the basis of anisotropic linear elasticity [16]. As seen in Table II, σ_P^{corr} converges more rapidly with unit cell size and leads to a Peierls stress of about 2.8 GPa for pure W. With quantum ESPRESSO we obtain the slightly lower value of 2.5 GPa which we attribute to the somewhat different methodology. These results lie within a range of values which have been obtained in previous investigations for W using different types of BOPs [20,21].

VCA calculations show a gradual decrease of the Peierls stress with increasing Re content (Table II). Note that for asymmetric core structures, negative or positive strain can lead to different Peierls stresses. At $c = 0.25$ we found, however, a very similar value of $\sigma_P^{\mathrm{corr}} = 1.78(10)$ GPa when reversing strain. Experimentally σ_P has been found to amount to 1.58, 1.41, 1.01, and 0.66 GPa for $c = 0$, 0.02, 0.07, and 0.25, respectively [3]. The absolute values of the experimental Peierls stresses are consistently lower than the theoretical ones which is a quite general phenomenon [30]. However, the experimental values show a consistent decrease of σ_P in good agreement with our calculations. The reason for the reduction in Peierls stress is most likely not the symmetric to asymmetric transition as previous studies [26] have shown that asymmetric cores tend to lead to higher σ_P as compared to symmetric ones when keeping elastic properties constant. We rather attribute the effect to the reduced resistance in shear occurring due to Re alloying as we observed before. This is also consistent with what has been proposed in Refs. [2,5] by means of more general arguments based on filling of the d band.

In conclusion, our DFT calculations show that alloying Re into W modifies the basic properties of the $1/2\langle 111\rangle$ screw dislocation. It leads to a transition from a symmetric to an asymmetric core and to a reduction in Peierls stress. This implies a change in the preferred slip plane and softening of the alloy as is observed experimentally. These two findings are crucial for the Re ductilization effect as the former increases the number of available slip planes and the latter reduces the stress level required to initiate plastic deformation. Hence, our calculations demonstrate that the origins for this effect are intrinsic to the alloy and stem from the filling of the d band which modifies the interatomic bonding. Because of their isoelectronic structures, similar results for the other group VIA metals, Cr and Mo, can be expected.

This work is supported by the EU through the EURATOM program. The views and opinions expressed herein do not necessarily reflect those of the European Commission.

*lorenz.romaner@mu-leoben.at

[1] G. A. Geach and J. E. Hughes, *Plansee Proceedings* (Pergamon, New York, 1956).
[2] W. D. Klopp, NASA TN **D-4955**, 1 (1968).
[3] P. L. Raffo, J. Less-Common Met. **17**, 133 (1969).
[4] A. Gilbert, M. J. Klein, and J. W. Edington, NASA CR **81225**, 1 (1966).
[5] A. Luo, D. L. Jabobsen, and K. S. Shin, Int. J. Refract. Met. Hard Mater. **10**, 107 (1991).
[6] D. R. Trinkle and C. Woodward, Science **310**, 1665 (2005).
[7] N. I. Medvedeva, Y. N. Gornostyrev, and A. J. Freeman, Phys. Rev. Lett. **94**, 136402 (2005).
[8] M. Garfinkle, NASA TN **D-3190**, 1 (1966).
[9] L. Nordheim, Ann. Phys. (Leipzig) **401**, 607 (1931).
[10] K. Persson, M. Ekman, and G. Grimvall, Phys. Rev. B **60**, 9999 (1999).
[11] S. Baroni *et al.*, http://www.pwscf.org/ (2007).
[12] G. Kresse and J. Furthmüller, Comput. Mater. Sci. **6**, 15 (1996).
[13] R. A. Ayres, G. Shanette, and D. Stein, J. Appl. Phys. **46**, 1526 (1975).
[14] L. Ventelon and F. Willaime, J. Comput.-Aided Mater. Des. **14**, 85 (2007).
[15] D. E. Segall *et al.*, Phys. Rev. B **68**, 014104 (2003).
[16] W. Cai *et al.*, Phys. Rev. Lett. **86**, 5727 (2001).
[17] J. Li *et al.*, Phys. Rev. B **70**, 104113 (2004).
[18] M. S. Duesbery and V. Vitek, Acta Mater. **46**, 1481 (1998).
[19] V. Vitek, Cryst. Lattice Defects **5**, 1 (1974).
[20] R. Gröger, A. Bailey, and V. Vitek, Acta Mater. **56**, 5401 (2008).
[21] M. Mrovec *et al.*, Phys. Rev. B **75**, 104119 (2007).
[22] V. Vitek, Philos. Mag. **84**, 415 (2004).
[23] J. P. Hirth and J. Lothe, *Theory of Dislocations* (Wiley-Interscience, New York, 1982).
[24] C. Woodward, Mater. Sci. Eng. A **400–401**, 59 (2005).
[25] Takeuchi, Philos. Mag. A **39**, 661 (1979).
[26] G. Wang, A. Strachan, T. Çagın, and W. A. Goddard, Phys. Rev. B **67**, 140101(R) (2003).
[27] S. Ismail-Beigi and T. A. Arias, Phys. Rev. Lett. **84**, 1499 (2000).
[28] C. Woodward and S. I. Rao, Phys. Rev. Lett. **88**, 216402 (2002).
[29] S. L. Frederiksen and K. W. Jacobsen, Philos. Mag. **83**, 365 (2003).
[30] R. Gröger and V. Vitek, Philos. Mag. Lett. **87**, 113 (2007).